View metadata, citation and similar papers at core.ac.uk

brought to you by CORE

provided by Elsevier - Publisher Connector

Available online at www.sciencedirect.com

ScienceDirect

Energy Procedia 79 (2015) 278 – 283

Energy Procedia

2015 International Conference on Alternative Energy in Developing Countries and Emerging Economies

Development of Kinetics Models in Each Zone of a 10 kg/hr Downdraft Gasifier using Computational Fluid Dynamics

Pubet Meenaroch[a*], Somrat Kerdsuwan[a], Krongkaew Laohalidanond[a]

[a]*The Waste Incineration Research Center, Department of Mechanical and Aerospace Engineering, Faculty of Engineering, Science and Technology Research Institute, King Mongkut's University of Technology North Bangkok, Bangkok, 1800, Thailand*

Abstract

In order to optimize the operating conditions of a downdraft gasification process, mathematical models are commonly used to reduce the expenditure occurring during the experimental work. This study aims to develop a kinetics model to demonstrate the gasification process in each zone of a 10 kg/hr downdraft gasifier, including drying, pyrolysis, oxidation, and reduction zone. Computational fluid dynamics (CFD) is used to solve the partial differential equations. The Euler-Lagrange approach for dispersed two-phase flows has been applied for simulating the gas-solid transport phenomena inside the gasifier. The results of this study include the effect of air flow rate on the temperature profile along the height of the gasifier and the concentration of producer gas at the gasifier outlet. Model validation has been made with experiments using wood chips as feedstock.

© 2015 The Authors. Published by Elsevier Ltd. This is an open access article under the CC BY-NC-ND license (http://creativecommons.org/licenses/by-nc-nd/4.0/).

Peer-review under responsibility of the Organizing Committee of 2015 AEDCEE

Keywords: Renewable energy, Downdraft gasification, Computational fluid dynamics, Kinetics model

1. Introduction

Nowadays, the residual biomass from agricultural products has been increasing significantly and is left without use or is inefficient. Studying the properties of biomass, it has been found that it is high in volatile matter, low sulphur, and ash content, which can be used as an alternative energy source to solve the current energy crisis [1]. The gasification process is a thermal-chemical conversion technology which is suitable for converting biomass into producer gas, consisting of CO, H_2, and CH_4. The producer gas can be used as fuel in internal combustion engines to generate electricity. This study focused on the downdraft

* Corresponding author. Tel.: +0-662-555-2000; fax: +0-662-555-2000
E-mail address: iampubet@gmail.com

1876-6102 © 2015 The Authors. Published by Elsevier Ltd. This is an open access article under the CC BY-NC-ND license (http://creativecommons.org/licenses/by-nc-nd/4.0/).

Peer-review under responsibility of the Organizing Committee of 2015 AEDCEE
doi:10.1016/j.egypro.2015.11.485

gasifier because it can produce low tar producer gas and it can be established within the community for decentralized electricity production [2].

Since the reactions occurring in the gasification process are very complex, the operating conditions have influences on both the producer gas quantity and quality. In order to reduce time and expense during the experimental work, mathematic models of the gasification process were developed. I. Janajreh and M. Al Shrah improved the kinetics model and used 2D-CFD for predicting the temperature distribution in the downdraft gasifier and the evolution of the producer gas [3].

The objective of this study was to develop a kinetics model of a 10 kg/hr lab-scale downdraft gasifier. The gasification models can predict the gas-solid transport phenomena and the kinetics reactions in each zone of the reactor consisting of the pyrolysis, oxidation, and reduction zone. The model results showed the effects of the air flow rate on the temperature profile along the height of the gasifier and the concentration of producer gas at the outlet. In addition, the model results were compared to the experimental data from a previous study using wood chips as feedstock in downdraft gasifier.

2. Computational model

2.1. Geometry and assumptions

The geometry of a lab-scale downdraft gasifier is given in Fig 1. The inner diameter and the height of cylindrical gasifier were 0.268 m and 0.8 m, respectively. The air was injected 0.5 m from the top of the gasifier. The total number of quadrilateral mesh cells was 10,744 elements.

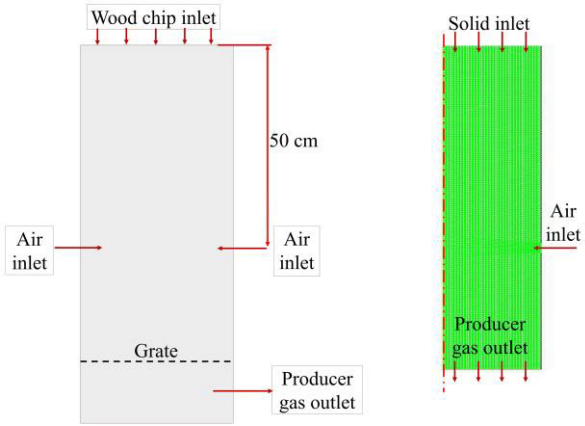

Fig. 1. Schematic of the downdraft gasifier and 2D axisymmetric geometry of a lab-scale downdraft gasifier

Downdraft gasification processes are very complex because of the transport phenomena between the gas-solid phases. Therefore, in order to simplify the simulation the following assumptions were used:

- 2D axisymmetric and steady state (the temperature distribution and the concentration of producer gas remained unchanged with time)
- No-slip boundary condition was assumed on the wall of gasifier. The wall was assumed to be insulated and therefore the heat flux on the wall was neglected.
- The feedstock fed at the top of gasifier was spherical and of uniform size. The particle size was smaller than 0.1 mm according to the limitation of the discrete phase model.

2.2. Model equations

The governing equations for continuity, momentum, energy, turbulent kinetic energy (k), turbulent dissipation rate (ε), and species transport equation were applied to solve for the continuous phase. The discrete phase model was applied to wood particles flow. The coupling between the discrete and gas phase which was added as source terms for the governing equations was the interphase exchange of mass, momentum, and energy. The discrete phase model are listed in Table 1.

Table 1. Discrete phase model

Discrete phase model	
Force balance: $\frac{\partial \vec{u}_p}{\partial t} = F_D\left(\vec{u} - \vec{u}_p\right) + \frac{\vec{g}\left(\rho_P - \rho\right)}{\rho_P}$	(1)
Inert heating and cooling: $m_p c_p \frac{dT_p}{dt} = hA_p\left(T - T_p\right) + \varepsilon_p A_p \sigma\left(\theta_R^4 - T_p^4\right)$	(2)
The single kinetic rate model: $-\frac{dm_p}{dt} = k_v\left(m_p - (1 - f_{v,0})(1 - f_{w,0})m_{p,0}\right)$	(3)
Heat transfer during devolatilizaion process: $m_p c_p \frac{dT_p}{dt} = hA_p\left(T - T_p\right) + \frac{dm_p}{dt} h_{fg} + \varepsilon_p A_p \sigma\left(\theta_R^4 - T_p^4\right)$	(4)
Heat transfer during the char combustion process: $m_p c_p \frac{dT_p}{dt} = hA_p\left(T - T_p\right) + f_h \frac{dm_p}{dt} H_{reac} + \varepsilon_p A_p \sigma\left(\theta_R^4 - T_p^4\right)$	(5)

2.3 Reaction models

The reaction models, e.g. moisture evaporation, devolatilization, heterogeneous surface reactions, and homogeneous reactions, were the source terms for the governing equations. The moisture evaporation in the drying zone was assumed to be controlled by droplet vaporization, which could be applied when the wood particle temperature reaches the vaporization temperature. The pyrolysis rate of the wood chips was controlled by kinetic reactions, which were described by Arrhenius equations. The pre-exponential factor (A) and the activation energy (E_a) for the reaction rate of the wood chip pyrolysis were 10^8 s^{-1} and 140 kJ/mol·K, respectively [4]. The reaction kinetics rate of the heterogeneous surface reactions (RC 1-5) and the homogeneous reactions (RG 1-3) are shown in Table 2.

Table 2. Kinetic reaction rate of heterogeneous surface reactions and the homogeneous reactions

	Reactions	A (*consistent unit*)	E (*kJ/mol*)	Temperature exponent	Reference
RC-1	$C + O_2 \rightarrow CO_2$	5.67e+09	160	0	[4]
RC-2	$2C + O_2 \rightarrow 2CO$	7.92e+04	218	0	[4]
RC-3	$C + CO_2 \rightarrow 2CO$	5.89e+02	222.8	1	[5]
RC-4	$C + 2H_2 \rightarrow CH_4$	1e+11	42	0	[4]
RC-5	$C + H_2O \rightarrow CO + H_2$	5.714	65.8	1	[5]
RG-1	$2CO + O_2 \rightarrow 2CO_2$	1.3e+11	125.6	0	[5]
RG-2	$2H_2 + O_2 \rightarrow 2H_2O$	3.53e+8	30.5	0	[5]
RG-3	$CO + H_2O \rightarrow CO_2 + H_2$	0.0265	65.8	0	[4]

2.4 Boundary conditions

The boundary conditions for the simulation of the 2D-CFD model of the lab-scale downdraft gasifier were similar to the operating conditions of the previous experiment. The air flow rate was varied from 250 to 450 L/min. The mass flow rate of wood particles was 10 kg/hr. The initial temperature of wood chips and air was 300 K [9]. The properties of the wood chips were composed of 20.10 % moisture, 67.84 % volatile matter, 11.58 % fixed carbon, 0.48 % ash (as received basis). The empirical formula of wood chips was calculated by using ultimate analysis (50.53 %C, 1.57 %H, 47.89 %O, and 0.01 %N) [6].

3. Results and discussion

3.1. Comparison between the simulation results and the experimental results

The results of the mathematical model were compared to the experimental results [6] for the same condition; in this case, the simulation of the air flow rate of 400 L/min was taken into consideration.

Table 3. Comparison of the simulation temperature distribution results with the experimental values

Thermocouple point	Experimental temperature results (K) [6]	Simulation temperature results (K)	% deviation
T1	1075	1279	18.98
T2	1068	1304	22.10
T3	1329	1325	0.30
T4	1165	1187	1.89
T5	602	672	11.63
T6	423	495	16.78

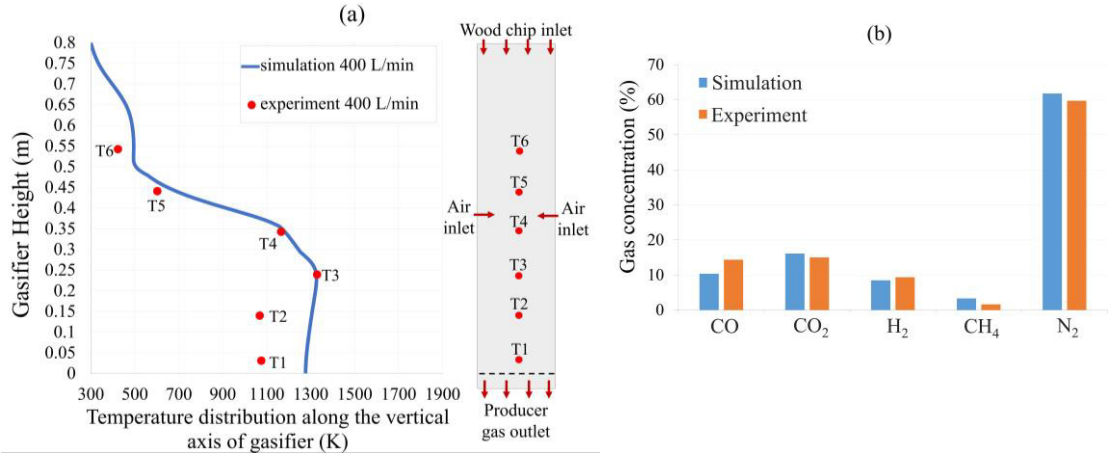

Fig. 2. (a) Simulation and experimental result of temperature distribution; (b) Simulation and experimental results for the producer gas composition

According to Fig 2 (a) and Table 3, the simulation results were similar to the experimental results at thermocouple No. 3, 4, and 5, corresponding to the deviation of 0.30, 1.89, and 11.63, respectively. At

thermocouple No. 1, 2, and 6, the simulation results were drastically different from the experimental results. The main reason for the significant deviation at the bottom of the gasifier was the continuous feeding of the wood chips assumed in this simulation. This continuous feeding led to a high gas yield and, consequently, enhanced the heat transfer throughout the reactor.

Fig 2 (b) shows the predicted producer gas compositions compared to those from experimental results. The producer gas consisted of combustible gases (CO, H_2, and CH_4) and incombustible gases (CO_2, and N_2). The predicted and experimental results for the producer gas concentration were similar. The predicted CO concentration was 10.35 % by mole, which was 4 % lower than the experimental value. The simulation results for the CO_2, H_2, and CH_4 concentration were accurate because their deviations were less than 1.7 %. These models yielded good agreement between the simulation and experimental results. Therefore, the models were further used to predict the influence of different air flow rates on temperature distribution and composition of producer gas.

3.2 Comparison of the influence of the air flow rate on temperature distribution and producer gas compositions

In order to study the effect of air flow rate on temperature distribution and producer gas composition, the air flow rate into the gasifier was varied from 250 to 450 L/min with the interval of 50 L/min.

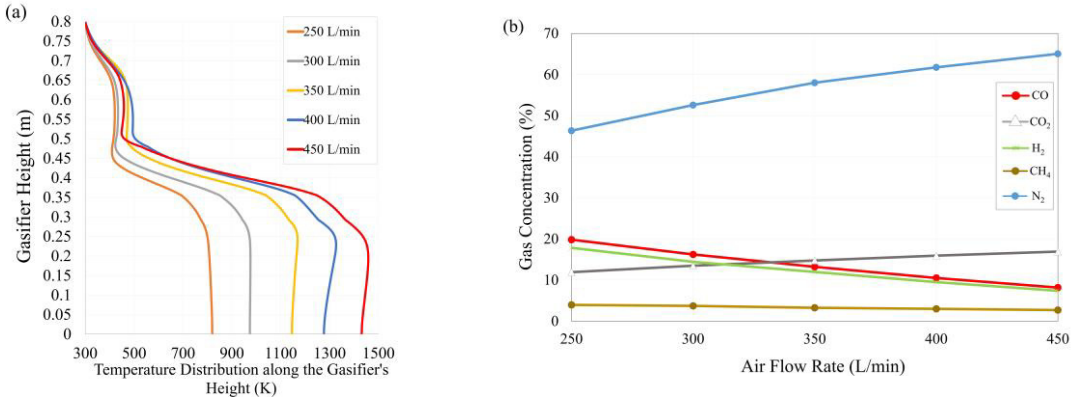

Fig. 3. (a) The effect of air flow rate on temperature distribution along the gasifier's height; (b) The effect of air flow rate on the producer gas composition

Fig 3 (a) shows the simulation results for the temperature distribution along the gasifier's height at different air flow rates. While the air flow rate increased from 250 to 300 L/min, the drying zone was between 0.44 to 0.80 m. Moreover, if the air flow rate was increase further (from 350 to 450 L/min), the drying zone changed to between 0.60 to 0.80 m. The drying zone had an approximate temperature under 473 K. In order to explicitly observe the combustion and reduction zone, an increase of the air flow rate from 350 to 450 L/min was explained. The approximate maximum temperature when running with an air flow rate of 350, 400, and 450 L/min was 1169, 1326, and 1458 K, respectively, which took place at the gasifier height of 0.20 - 0.24 m. In the regime of the reduction zone between 0 m and the peak temperature point, the temperature slightly dropped to approximately 23, 48, and 27 K at the air flow rate of 350, 400, and 450 L/min, respectively. In addition, an increase in the temperature distribution resulted from an increase of the air flow rate and increased the O_2 concentration in the combustion zone, which facilitated the char combustion reaction rate (RC-1) and volatile combustion reaction rate (RG-1, RG-2).

Fig 3 (b) presents the mole fraction of the producer gas compositions at different air flow rates. While the air flow rate increased from 250 to 450 L/min, the mole fraction of CO_2 increased from 11.06 to 17.00 % by mole. This increase in CO_2 concentration can be explained by reactions RC-1 and RG-1. The more O_2 could react with the CO and char to produce CO_2. Considering CO the in producer gas, its concentration decreased with the increasing air flow rate from 20.8 to 8.04 % by mole because the incomplete combustion reaction rate (RC-2) decreased. Moreover, the air flow rate affected the H_2 contained in the producer gas, as it decreased with increasing air flow rates. This is the result of the increase in the H_2 combustion reaction (RG-2).

4. Conclusion

The Euler-Lagrange approach for disperse flow was applied for simulating gas-solid transport phenomena inside a 10 kg/hr lab-scale downdraft gasifier. The effect of air flow rate on the temperature distribution along the height of the gasifier and the producer gas composition at the exit were investigated and compared to the experimental results of the previous work using wood chips as feedstock.

The simulation results showed that the temperature distribution inside the gasifier increased with an increase in the air flow rate. These results can be explained because of the increase of the increase in the char combustion reaction rate and volatile combustion reaction rate.

Regarding the producer gas composition, an increase in air flow rate led to a decrease in CO and H_2 concentration, whereas the CO_2 increased. The reason was the increase in the O_2 concentration in the air introduced into the gasifier, which facilitated the char combustion reaction rate and H_2 combustion reaction rate to increase. The developed model can be used to optimize the running parameters of a downdraft gasifier to archive optimum cold gas efficiency.

Acknowledgements

The authors would like to thank the Development of Machinery and Industrial Equipment (DMIE), Science and Technology Research Institute, for supporting the FLUENT program, and the Waste Incineration Research Center (WIRC) as well as the Department of Mechanical and Aerospace Engineering (MAE), Faculty of Engineering, King Mongkut's University of Technology North Bangkok, for their kind cooperation.

References

[1] Anjireddy, Bhavanam, R. C. Sastry. Biomass Gasification Processes in Downdraft Fixed Bed Reactors. *International Journal of Chemical Engineering and Applications*. 2011:**6;**425-433.

[2] P. Abdul Salam, S. Kumar, Manjula Siriwardhana. The Status of Biomass Gasification in Thailand and Cambodia. *Energy Environment Partnership*. 2010;6-12.

[3] I. Janajreh and M. Al Shrah. Numerical and Experimental Investigation of Downdraft Gasification of Wood Chips. *Energy Conversion and Management*. 2013;**65**:783–792.

[4] Colomba Di Blasi. Dynamic Behaviour of stratified downdraft gasifiers. *Chemical Engineering Science*. 2000;**55**:2931–44.

[5] Yueshi Wu, Qinglin Zhang, Weihong Yang, W. Blasiak. Two-Dimensional Computational Fluid Dynamics Simulation of Biomass Gasification in a Downdraft Fixed-Bed Gasifier with Highly Preheated Air and Steam. *Energy Fuels*. 2013;**27**:3274-3282.

[6] Nimit Nipattummakul, Suthum Patumsawad, Somrat Kerdsuwan. *An Experimental investigation of a 15 kg/hr Downdraft Gasifier for Power Generation*. ICEE. Songkhla; 2007.